

LYMPHOID NEOPLASIA

Intracellular NAD⁺ depletion enhances bortezomib-induced anti-myeloma activity

Antonia Cagnetta,^{1,2} Michele Cea,^{1,2} Teresa Calimeri,¹ Chirag Acharya,¹ Mariateresa Fulciniti,¹ Yu-Tzu Tai,¹ Teru Hideshima,¹ Dharminder Chauhan,¹ Mike Y. Zhong,¹ Franco Patrone,³ Alessio Nencioni,³ Marco Gobbi,² Paul Richardson,¹ Nikhil Munshi,¹ and Kenneth C. Anderson¹

¹LeBow Institute for Myeloma Therapeutics and Jerome Lipper Multiple Myeloma Center, Dana-Farber Cancer Institute, Harvard Medical School, Boston, MA; and ²Department of Hematology and Oncology, and ³Departments of Internal Medicine, Istituto Di Ricovero e Cura a Carattere Scientifico Azienda Ospedaliera Universitaria San Martino-IST, Genova, Italy

Key Points

- FK866 combined with bortezomib induces synergistic anti-MM cell death.
- Addition of low doses of NAD⁺-depleting agent FK866 overcomes bortezomib resistance in MM cells.

We recently demonstrated that Nicotinamide phosphoribosyltransferase (Nampt) inhibition depletes intracellular NAD⁺ content leading, to autophagic multiple myeloma (MM) cell death. Bortezomib has remarkably improved MM patient outcome, but dose-limiting toxicities and development of resistance limit its long-term utility. Here we observed higher Nampt messenger RNA levels in bortezomib-resistant patient MM cells, which correlated with decreased overall survival. We demonstrated that combining the NAD⁺ depleting agent FK866 with bortezomib induces synergistic anti-MM cell death and overcomes bortezomib resistance. This effect is associated with (1) activation of caspase-8, caspase-9, caspase-3, poly (ADP-ribose) polymerase, and downregulation of Mcl-1; (2) enhanced intracellular NAD⁺ depletion; (3) inhibition of chymotrypsin-like, caspase-like, and trypsin-like proteasome activities; (4) inhibition of nuclear factor κ B signaling; and (5) inhibition of angiogenesis. Furthermore, Nampt knockdown significantly enhances the

anti-MM effect of bortezomib, which can be rescued by ectopically overexpressing Nampt. In a murine xenograft MM model, low-dose combination FK866 and Bortezomib is well tolerated, significantly inhibits tumor growth, and prolongs host survival. Taken together, these findings indicate that intracellular NAD⁺ level represents a major determinant in the ability of bortezomib to induce apoptosis in MM cells and provide proof of concept for the combination with FK866 as a new strategy to enhance sensitivity or overcome resistance to bortezomib. (*Blood*. 2013;122(7):1243-1255)

Introduction

A prominent feature of malignant cells is the acquisition of characteristics that enable uncontrolled proliferation, including the capability to modify or reprogram cellular metabolism.¹⁻³ In such a scenario, tumor cells exhibit highly increased rates of energy-consuming reactions due to elevated intracellular NAD⁺ levels, with pyridine nucleotide linking bioenergetic processes and signaling pathways mediating tumor cell growth and survival.⁴⁻⁶ This realization has provided the basis for molecular studies of NAD⁺ metabolism to identify novel targeted therapeutic strategies. Recently, we demonstrated that Nicotinamide phosphoribosyl transferase (Nampt), a key enzyme involved in NAD⁺ metabolism, is essential for maintenance of multiple myeloma (MM) cell viability and conversely, that Nampt inhibition/depletion potently kills MM cells.^{7,8} Importantly, the chemical inhibitor of Nampt FK866 induced cell death in MM cells sensitive to and resistant to conventional and novel therapies. By depleting intracellular NAD⁺-levels, FK866 triggers autophagic MM cell death via transcriptional-dependent (transcription factor EB) and -independent (PI3K-MTORC1) mechanisms. In vivo studies in murine xenograft models of human

MM showed that FK866 is well tolerated, prolongs survival, and reduces tumor growth. Numerous studies in other cancers have also revealed promising results by combining NAD⁺-depleting agents with TRAIL,⁹ DNA damaging agents (daunorubicin, cisplatin, Ara-C, and melphalan),¹⁰⁻¹² and ionizing radiation.¹³

Proteasome inhibitor bortezomib has transformed therapy of relapsed MM, as well as prolonged event-free and overall survival when used as initial therapy for newly diagnosis disease.¹⁴ However, prolonged bortezomib exposure may result in cumulative toxicity and acquisition of drug resistance.¹⁵ Combination approaches aimed to prevent or overcome mechanism(s) of bortezomib resistance offer great potential to improve outcome. For example, preclinical and clinical studies suggest that induction of aggresomal protein degradation is a mechanism of resistance to bortezomib and conversely, that adding histone deacetylase inhibitor to block aggresomal protein degradation can restore response to bortezomib.¹⁶

In the present study, our gene expression profile analysis of publically available databases (GSE9782) revealed significantly higher Nampt messenger RNA (mRNA) levels in patients with

Submitted February 7, 2013; accepted June 8, 2013. Prepublished online as *Blood* First Edition paper, July 3, 2013; DOI 10.1182/blood-2013-02-483511.

A.C. and M.C. contributed equally to this study.

Presented in part as an oral communication at the American Society of Hematology Annual Meeting, Atlanta, GA, December 2012.

The online version of this article contains a data supplement.

The publication costs of this article were defrayed in part by page charge payment. Therefore, and solely to indicate this fact, this article is hereby marked "advertisement" in accordance with 18 USC section 1734.

© 2013 by The American Society of Hematology

relapsed MM who did not respond to bortezomib in comparison with responders; moreover, Nampt levels correlated with overall survival. These findings prompted us to investigate the anti-MM effect of Nampt inhibitor FK866 combined with bortezomib in a panel of MM cell lines and patient MM cells sensitive and resistant to bortezomib. Both in vitro and in our in vivo MM xenograft models, combination therapy triggers synergistic anti-MM activity and overcomes bortezomib resistance. Furthermore, Nampt knockdown overcomes bortezomib resistance, which can be rescued by Nampt overexpression. Overall our data provide the rationale for combining FK866 with bortezomib to enhance sensitivity or overcome resistance to bortezomib and thereby improve patient outcome.

Methods

For a more detailed description of the methods used, see the supplemental Methods section on the *Blood* Website.

Cell lines

Cell lines were obtained from the American Type Culture Collection (Manassas, VA) or were kindly provided by sources indicated in the supplemental Methods section.

Gene expression and survival analysis

We evaluated the expression levels of Nampt transcript (probe ID 217739_s_at) in the log₁₀ transformed data set downloaded from the National Center for Biotechnology Information's (Bethesda, MD) gene expression omnibus database (Millennium Pharmaceuticals, Cambridge, MA; series number GSE9782) of tumor cells from MM patients after their enrollment in phases 2 and 3 trials evaluating bortezomib or dexamethasone treatment of relapsed MM. The bortezomib-responder (n = 85) and not-responder (n = 78) populations within each therapy group were compared using the Student *t* test to determine statistical significance. The correlation of Nampt transcript levels with clinical outcome was measured by evaluating its expression levels in tumor cells from all bortezomib-treated patients (n = 163) with a median-centered gene expression data set. Patients were classified as having high versus low levels of Nampt, and Kaplan–Meier survival analysis comparing the 2 groups was carried out by GraphPad Prism 5.0 (La Jolla, CA).

In vitro capillary-like tube structure formation assay

The drug effects on angiogenesis were studied using an in vitro Angiogenesis Assay Kit (Chemicon International, Billerica, MA). Human umbilical vein endothelial cells (HUVECs) were cultured in endothelial growth media (Lonza, Walkersville, MD), supplemented with a cocktail of growth factors, according to the manufacturer's instructions. HUVECs were harvested; resuspended in endothelial growth medium (Cambrex, East Rutherford, NJ) with vehicle, FK866 (10 nM), bortezomib (2.5 nM), or their combination; and then added to a plate containing matrigel (10,000 cells/well). After 8 hours, tube formation was evaluated using a Nikon (Tokyo, Japan) inverted TE2000 microscope, and images were captured by Orca ER digital CCD camera (Hamamatsu Photonics, Hamamatsu City, Japan), as described.¹⁷

Immunoblotting

MM cells were cultured with or without stimuli, harvested, washed, and lysed using radioimmunoprecipitation assay buffer. Proteins were separated on a sodium dodecyl sulfate–polyacrylamide gel and electroblotted on a polyvinylidene difluoride membrane (Pall Gelman Laboratory, Ann Arbor, MI). Proteins were visualized by probing the membranes with the following antibodies: anti-tubulin, -ubiquitin, -caspase-3, -caspase-8, -caspase-9, -poly (ADP-ribose) polymerase (PARP), -Bcl-2, -Mcl-1, -p-p65, -p-p52, -RelB, -p-IkB, and -nucleolin (Cell Signaling Technology, Beverly, MA); anti-Nampt (Bethyl Laboratories, Montgomery, TX); and anti-glyceraldehyde 3-phosphate

dehydrogenase (GAPDH) and -actin (Santa Cruz Biotechnology, Dallas, TX). Standard enhanced chemiluminescence was used for protein band detection.

Transfection assays

Nampt knockdown experiment was performed using short hairpin RNA (shRNA) sequences and a lentivirus-mediated shRNA delivery, as previously described.⁷ The ectopic Nampt overexpression was performed using hNampt/pcDNA or pcDNA empty vector (kindly provided by David A. Sinclair, Harvard Medical School, Boston, MA).¹¹ MM1S and U266 cells were transfected with hNampt/pcDNA or pcDNA empty vector using the cell line Nucleofector Kit V or C solution (Amaxa Biosystems, Lonza, Basel, Switzerland), respectively, as per the manufacturer's instructions. MM cells depleted or overexpressing Nampt were then treated with low doses of bortezomib (1.25–5 nM) for 48 hours, and their viability was analyzed by propidium iodide (PI) staining and fluorescence-activated cell sorter (FACS) assays.

Murine xenograft model of human MM

CB17–severe combined immunodeficiency (SCID) mice (28–35 days old) were purchased from Charles River Laboratories (Wilmington, MA). All animal studies were conducted according to protocols approved by the Animal Ethics Committee of the Dana-Farber Cancer Institute. Mice were irradiated (200 cGy) and then inoculated subcutaneously in the right flank with 5×10^6 MM1S cells in 100 μ L RPMI 1640. Following detection of tumor (~3 weeks after the injection), mice (n = 7 group) were treated intraperitoneally with FK866 (30 mg/kg body weight) daily for 4 days, repeated weekly over 3 weeks; bortezomib 0.5 mg/kg dissolved in 0.9% saline solution biweekly (subcutaneous) for 3 consecutive weeks; or the combination with the same dosing regimen used for the individual agents. The control group received the carrier alone at the same schedule as the combination group. Caliper measurements of the longest perpendicular tumor diameters were performed twice a week to estimate the tumor volume using the following formula: length \times width² \times 0.5. Tumor growth inhibition was calculated using the formula $(\Delta_{\text{control average volume}} - \Delta_{\text{treated average volume}}) \times 100 (\Delta_{\text{control average volume}})$. Animals were sacrificed when tumors reached 2 cm³ or the mice appeared moribund. Survival was evaluated from the first day of treatment until death.

Statistical analysis

Statistical significance of differences observed between drug-treated and control mice (in both in vitro and in vivo experiments) was determined by Student *t* test; differences were considered significant when $P \leq .05$. Tumor growth inhibition and Kaplan–Meier survival analysis were determined using GraphPad Prism analysis software. Drug synergism was analyzed by isobologram analysis using the CalcuSyn Version 2.0 software program (Biosoft, Palo Alto, CA). A combination index (CI) less than 1.0 indicates synergism; CI = 1, additive effect; and CI > 1, no significant combination effect.¹⁸

Results

Nampt protein is predominantly expressed in the cytoplasm of MM cells, and its expression correlates with clinical response to bortezomib

We have previously demonstrated significantly higher expression of Nampt in MM cell lines and patients' cells in comparison with healthy peripheral blood mononuclear cells (PBMCs), suggesting that its activity may play a role in MM cell growth and function.^{7,9} To gain further insight into activity of this protein, we first characterized its subcellular distribution in MM cells. Immunofluorescent studies using MM cell lines as well as patient cells, both sensitive and resistant to bortezomib, showed higher Nampt expression in the cytoplasm than in nuclei (Figure 1A). Similar results were observed using protein extracts from MM cell lines and mononuclear cells from MM patients (Figure 1B). In contrast, Nampt protein was equally

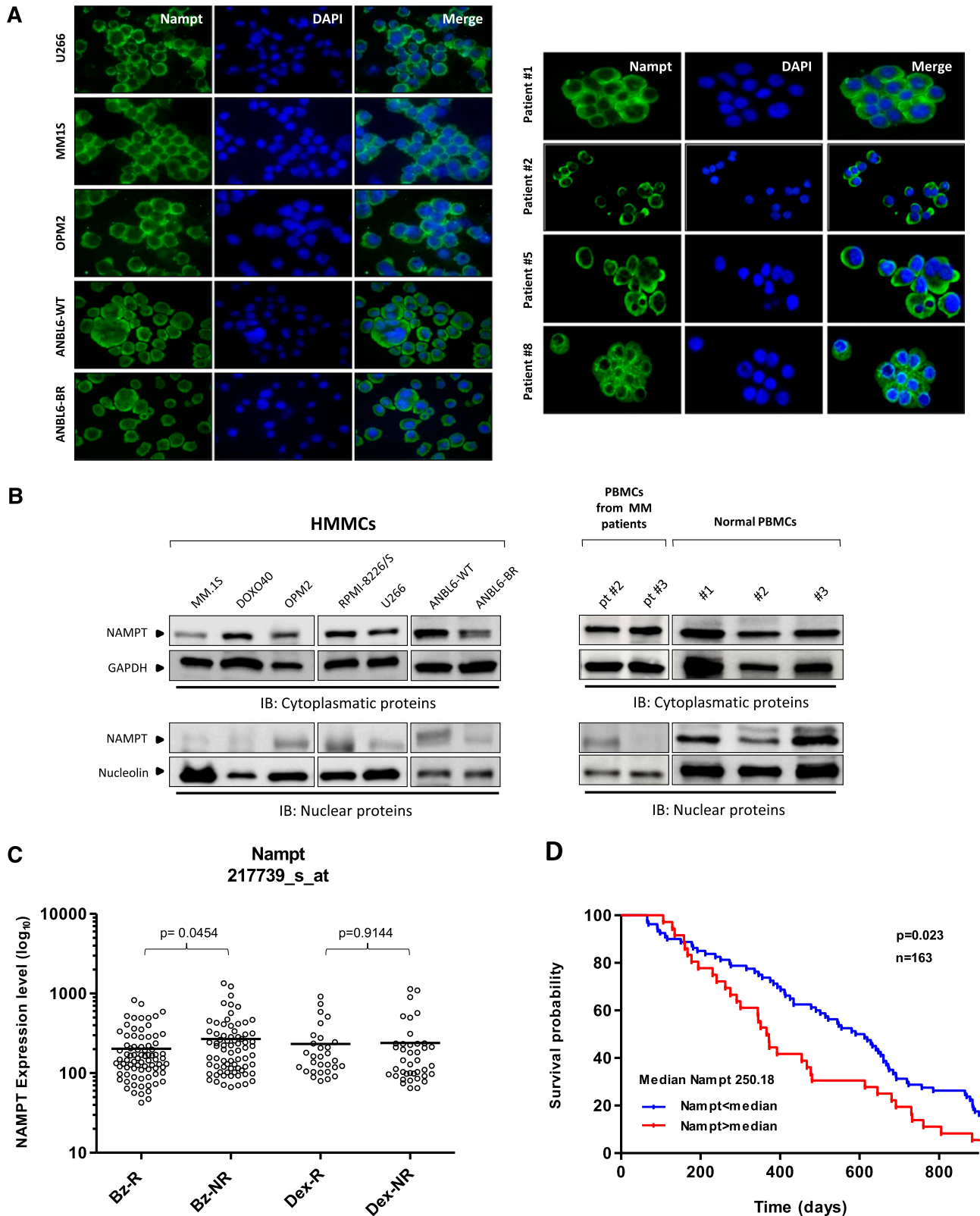


Figure 1. Nampt is a cytoplasmic protein with prognostic relevance in bortezomib-treated MM patients. (A-B) MM cell lines, MM patients' CD138⁺ cells, and PBMCs from healthy donors or MM patients were used to characterize subcellular distribution patterns of Nampt expression by immunofluorescence (A) or western blot analysis (B) using anti-Nampt and specific antibodies. (C) Expression levels (\log_{10} transformed) for Nampt transcript in CD138⁺ cells from MM patients after bortezomib (n = 163) or dexamethasone (n = 70) therapy, according to gene expression profile arrays generated at Millenium Pharmaceuticals (GSE9782). Nampt expression levels (Affimetrix probeset 217739_s_at) among responders (R) or nonresponders (NR) within Bz (n = 85 for R and n = 78 for NR) or Dex (n = 30 for R and n = 40 for NR) groups were plotted on the horizontal axis against the \log_{10} -transformed normalized expression units on the vertical axis. For each therapy group, P values comparing R and NR are shown. (D) Kaplan-Meier overall survival curves of MM patients treated with bortezomib (n = 163) according to Nampt mRNA expression above or below the median value of 250.18, based on gene expression omnibus dataset GSE9782. The blue line indicates a patient group with lower Nampt expression and longer survival, whereas the red line represents a group of patients with higher Nampt expression and shorter survival. Bz, bortezomib; DAPI, 4,6 diamidino-2-phenylindole; Dex, dexamethasone; HMMCs, human multiple myeloma cell lines.

present in both cellular compartments in PBMCs derived from healthy donors. Consistent with this localization of Nampt and in concert with its prominent role in metabolism, we hypothesized that Nampt may inhibit proteasome activity, associated with cytosolic accumulation of proteins in MM cells. To examine this possibility, we first retrospectively evaluated the prognostic relevance of Nampt by integrating a publicly available gene expression data set of tumor cells collected from patients with relapsed MM after treatment with either bortezomib or high-dose dexamethasone.¹⁹ Among bortezomib-treated patients, Nampt transcript (probe set 217739_s_at) values were higher in nonresponders than in responders, whereas no correlation was observed between responders and nonresponders to dexamethasone (Figure 1C). Thus Nampt expression correlates negatively with response to bortezomib. Importantly, Nampt transcript levels also correlated with overall survival of 163 bortezomib-treated MM patients enrolled in this clinical trial, with a statistically significant inverse correlation between Nampt levels and overall survival (Figure 1D). Collectively, these data suggest that targeting Nampt may represent an innovative strategy to enhance sensitivity or overcome resistance to Bortezomib.

Targeting Nampt and proteasome activity triggers synergistic anti-MM activity

On the basis of our preliminary data, we selected concentrations of Nampt inhibitor FK866 and bortezomib with only modest single-agent MM cell cytotoxicity in order to assess their combined cytotoxicity. We pretreated RPMI8226, U266, MM1S, MM1R (Dex resistant), ANBL6/WT (bortezomib sensitive), and ANBL6/BR (bortezomib resistant) MM cells with increasing doses of FK866 (1–3 nM) for 48 hours; bortezomib, over a range of concentrations depending on specific 50% inhibition/inhibitory concentration (IC₅₀) for each cell line (eg, MM1S, RPMI, MM1R, and U266, 2.5–10 nM; ANBL6/WT and ANBL6/BR, 1.25–5 nM), was then added for an additional 48 hours, followed by assessment of cell viability by PI staining and flow cytometry analysis. Enhanced cytotoxicity of the combination treatment in comparison with either agent alone was observed in all MM cell lines (Figure 2A); Chou and Talalay analysis confirmed synergistic anti-MM activity of FK866 plus bortezomib, with a CI < 1.0 in all MM cell lines tested (supplemental Figure 1A-E).

Next we evaluated whether low doses of FK866 could potentiate bortezomib effect on purified tumor cells derived from patients with MM responsive (n = 5) or resistant (n = 6) to bortezomib (Table 1). As is shown in Figure 2B and supplemental Figure 1F, combination treatment significantly decreased viability of all patient MM cells analyzed, irrespective of bortezomib clinical response status. We also evaluated whether healthy PBMCs would similarly be affected by FK866 and bortezomib, alone or in combination. Figure 2C shows that neither single agent nor the combination triggered death of PBMCs, suggesting a favorable therapeutic index. Thus the addition of bortezomib to FK866 results in highly synergistic anti-MM activity; bortezomib's activity is not potentiated by FK866 in PBMCs, which have lower proteasome activity.^{20,21}

We next examined the molecular mechanism whereby low-dose combined treatment of FK866 and bortezomib triggers synergistic anti-MM cytotoxicity. These studies were performed at 24 hours to reduce the confounding effects of cell death induction at later time points.⁷ In our previous work, we observed that autophagy was associated with FK866-induced MM cell death,^{7,8} consistent with a switch from cytoprotective to cytotoxic autophagy.²² Surprisingly, the combination of FK866 plus bortezomib was unable to further increase the LC3B-II level induced by either agent alone, suggesting

that autophagy cannot explain the observed synergism (data not shown); moreover, the biochemical modulator of autophagy 3-methyl adenine (3-MA) failed to protect MM cells from cytotoxicity induced by the drug combination.

Because a previous study linked cell death induced by FK866 combined with cisplatin/etoposide to apoptosis in neuroblastoma cells,¹² we next examined whether FK866 added to bortezomib also triggered apoptosis in MM cells. Indeed, we observed that combining low doses of these drugs markedly increased proteolytic cleavage of caspase-3, caspase-8, caspase-9, and PARP in both bortezomib-sensitive and -resistant MM cell lines (Figure 3A). Moreover, a significant activation of caspase 3 (supplemental Figure 2A) and increased percentage of cells in the late phase of apoptosis (Figure 3B; supplemental Figure 2B) was observed after treatment with combined versus single-agent therapy. Pretreatment of MM cells with the pan-caspase inhibitor z-VAD-fmk significantly abrogates FK866 plus bortezomib-induced MM cell death, confirming apoptosis triggered by this combination (supplemental Figure 3). Combined treatment also resulted in a marked reduction in expression of antiapoptotic Mcl-1 protein both in bortezomib-sensitive and -resistant MM cell lines. In contrast, only a modest effect on Bcl-2 protein level was observed at this interval (Figure 3A). Together, these findings indicate that the FK866 plus bortezomib regimen is effective against bortezomib-resistant as well as bortezomib-sensitive MM cells and elicits similar changes in survival proteins.

Combined treatment overcomes the survival advantage conferred by the BM microenvironment and inhibits in vitro capillary-like tube formation

Interaction of MM cells with the bone marrow (BM) microenvironment confers growth, survival, and drug resistance in tumor cells.²³ Thus we next tested the effect of BM stromal cells (BMSCs) on sensitivity of MM cells to combined FK866 plus bortezomib treatment. MM1S cells were cocultured with BMSCs or incubated with or without IL-6 (10 ng/mL) or IGF-1 (100 ng/mL), and then treated with FK866, bortezomib, or both drugs for 72 hours; proliferation was then measured by thymidine uptake assay. As is shown in Figure 4A-B, the drug combination completely overcomes the protective effects of IL-6 and IGF-1, as well as coculture with BMSCs. Remarkably, no significant growth inhibition in BMSCs was observed. These findings suggest that low doses of FK866 enhance MM cytotoxicity of bortezomib in the BM milieu.

Angiogenesis within the BM microenvironment is associated with progression of MM^{24,25}; we therefore next investigated the anti-angiogenic activity of FK866 and bortezomib using an in vitro capillary-like tube structure formation assay. HUVECs pretreated with vehicle, FK866 (10 nM), bortezomib (2.5 nM), or the combination were seeded in 96-well plates coated with Matrigel and analyzed at 8 hours for tube formation using an inverted microscope. As is shown in Figure 4C, tubule formation was markedly decreased in the FK866 plus bortezomib-treated cells versus treatment with either agent alone ($P = .0001$, $n = 3$). Importantly, analysis of HUVECs viability ruled out the possibility that drug inhibition of tumor vasculature formation was due to a direct cytotoxic effect. Overall, these data show that FK866 plus bortezomib targets MM cells and angiogenesis in the BM microenvironment.

Role of Nampt in modulating response to bortezomib

The above in vitro results led us to investigate the role played by Nampt in the observed synergism using loss- and gain-of-function approaches in MM cells (Figure 5A-B). Nampt depletion by lentiviral

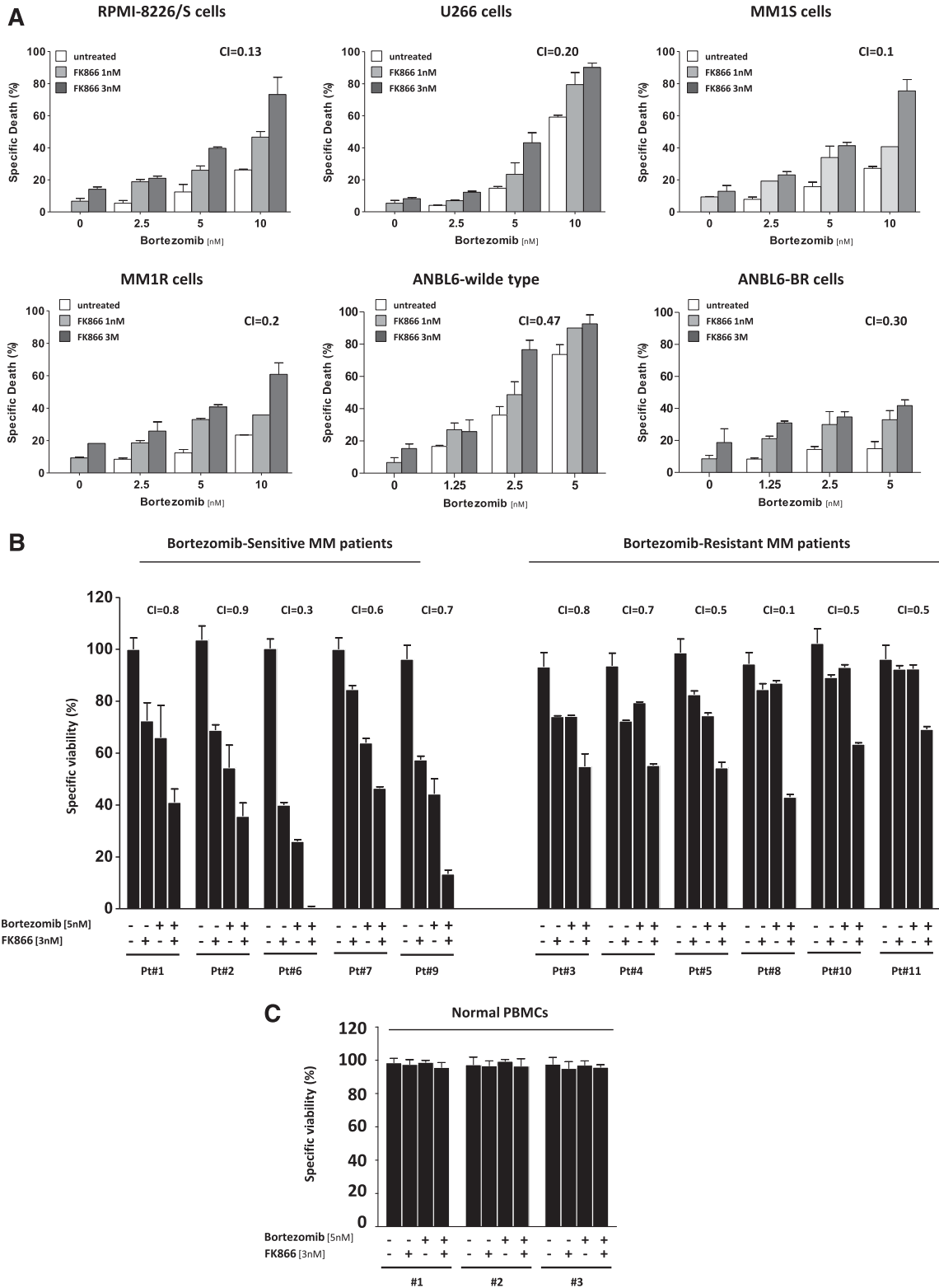


Figure 2. Combination of low doses of FK866 and bortezomib induces synergistic anti-MM activity. (A) RPMI-8226/S, U266, MM1S, MM1R ANBL6/WT, and ANBL6-BR cells were treated with or without increasing doses of FK866 (1–3 nM) for 48 hours, and then vehicle or bortezomib (over a range of concentrations depending on cell line) were added for a further 48 hours. Viability was assessed using PI staining and FACS analysis. Data presented are means of triplicate \pm SD ($n = 3$; $P < .05$ for all cell lines). CI values refer to the highest drug concentrations used. (B) Purified patient bortezomib-sensitive and -resistant MM (CD138⁺) cells were pretreated with FK866 for 48 hours; bortezomib was then added for an additional 48 hours, followed by cell death analysis using PI staining and FACS analysis. Data are mean \pm standard deviation (SD) of triplicate samples ($P < .05$ for all patient samples). A CI less than 1 indicates synergism. (C) PBMCs from healthy donors were treated as in panel B with indicated concentration of FK866, bortezomib, or their combination, and then analyzed for viability as described above.

Table 1. Clinical characteristics of MM patients

Patient no.	Disease status at time of sampling	Gender	Response to bortezomib	Bz (5 nM)	Specific viability ex vivo (%) FK866 (3 nM)	Combination (CI)
1	Diagnosis	M	Sensitive	66	72.4	41 (0.8)
2	Relapse	F	Sensitive	54.4	68.8	35.6 (0.9)
3	Relapse	M	Resistant	74.2	74.1	54.8 (0.8)
4	Refractory	F	Resistant	79.5	72.4	55.2 (0.7)
5	Refractory	F	Resistant	74.4	82.5	54.4 (0.5)
6	Relapse	F	Sensitive	26	40	0.5 (0.3)
7	Diagnosis	M	Sensitive	63.9	84.5	46.48 (0.6)
8	Relapse	M	Resistant	89.6	88	73.4 (0.1)
9	Relapse	M	Sensitive	57	44.5	13 (0.7)
10	Refractory	F	Resistant	93	89.1	63.4 (0.5)
11	Refractory	F	Resistant	92.4	92.4	69.2 (0.5)

Bz, bortezomib.

shRNA enhanced MM cell death upon treatment with bortezomib versus control (scrambled shRNA sequence), as is shown in Figure 5A. In contrast, its ectopic overexpression did not alter bortezomib-induced cell death in comparison with control. To formally define the role of Mcl-1 in the synergism of Nampt inhibition and bortezomib treatment, we analyzed the level of antiapoptotic protein Mcl-1 in U266 and MM1S cells following bortezomib treatment. As predicted, in cells depleted of Nampt, this treatment resulted in greater downregulation of Mcl-1 in comparison with scramble control, confirming the pivotal role of this proapoptotic protein in cell death triggered by these stimuli. Moreover, a weak effect on bcl-2 protein was also observed (Figure 5C).

As is well known, the effect of Nampt inhibition can be rescued by repletion of NAD⁺ through biosynthesis from Nicotinamide.²⁶ Here we found that exogenous Nicotinamide significantly rescued FK866 plus bortezomib-induced MM cell death, further confirming the pivotal role played by Nampt in bortezomib resistance and conversely, the role of Nampt inhibition in restoring anti-MM activity triggered by combination therapy (supplemental Figure 4).

Collectively, these studies demonstrate that Nampt inhibition combined with bortezomib mediates to the synergistic anti-MM activity.

Combined FK866 and bortezomib inhibits the UPS and NF- κ B pathways

We next explored the functional sequelae of this drug combination in MM cells using multiple biochemical and molecular assays. We first asked whether the main mechanism of FK866 action, namely, intracellular NAD⁺ depletion, contributes to the anti-MM effect of combined therapy. A cycling enzymatic assay showed that bortezomib alone, unlike low doses of FK866, was unable to reduce NAD⁺ levels in 3 different MM cell lines. Remarkably, the combination of FK866 plus bortezomib dramatically reduced intracellular NAD⁺ to undetectable levels in all MM cells analyzed, enhancing the metabolic consequences of FK866 treatment alone (Figure 6A). Because intracellular NAD⁺ and adenosine triphosphate (ATP) levels, whose depletion follows NAD⁺ shortage,^{12,27} share the capacity to affect proteasome enzymatic activity, we next turned our attention to a possible synergism at this level.

The proteolytic activity of proteasome is mediated by 3 active sites: chymotrypsin-like (CT-L), trypsin-like (T-L), and caspase-like (C-L).^{28,29} Previous studies showed that bortezomib primarily inhibits CT-L and, to a lesser degree, C-L activity.³⁰ Here we observed that treatment of MM1S cells for 6 hours with low-dose (2 nM) bortezomib inhibited 60% CT-L and 15% C-L activity, whereas FK866 (3 nM) for

48 hours inhibited only 40% CT-L and 3% C-L activities, as measured by activity assays using specific fluorogenic peptide substrates.³¹ Importantly, the combination of low doses of these drugs resulted in significant blockade of all 3 proteasomal activities (80%, 25%, and 15% inhibition of CT-L, C-L, and T-L, activities, respectively), as is shown in Figure 6B. Therefore, our findings suggest that the addition of FK866 significantly enhances the potency and selectivity of bortezomib against all proteasome activities and triggers potent anti-MM activity.

Bortezomib treatment results in the cytosolic accumulation of misfolded proteins targeted for degradation, thereby inducing downstream toxic effects leading to cell death. A more effective regulation of misfolded protein degradation is achieved by activating the ubiquitin–proteasome system (UPS).³² Therefore, we next tested whether the addition of FK866 to bortezomib affects the UPS. As is shown in Figure 6C, western blot analysis revealed a marked increase in ubiquitinated proteins after treatment with the combination of FK866 and bortezomib in comparison with low doses of either agent alone. Likewise, immunofluorescence analysis showed cytoplasmic accumulation of polyubiquitinated proteins when low-dose FK866 was added to bortezomib, to a greater extent than is noted after single-agent treatment (Figure 6D).

A broad spectrum of intracellular proteins are substrates for proteasome-mediated degradation in MM cells. For example, nuclear factor κ B (NF- κ B), a transcription factor that plays a pivotal role in growth and survival signaling in MM cells,^{30,33,34} forms complexes with the phosphorylated inhibitor of NF- κ B alpha (I κ B α), a proteasome substrate that prevents p65 nuclear translocation and activation of NF- κ B signaling. Furthermore, constitutive NF- κ B activity in patient MM cells renders cells refractory to bortezomib treatment,³⁵ with several reports showing deregulation of NF- κ B activity after treatment with either bortezomib^{30,33} or Nampt inhibitors.³⁶ We therefore next examined whether this drug combination affects NF- κ B signaling in MM cells to a greater extent than does either drug alone. By western blot analysis, we first evaluated protein levels in both canonical (p65 and p-I κ B) and noncanonical (p52 and RelB) NF- κ B pathways in MM cells treated with FK866, bortezomib, or the combination. As is shown in Figure 6E, tumor necrosis factor (TNF)- α -induced nuclear translocation of p65, p52, and RelB in MM cells was more significantly inhibited by the combination of FK866 and bortezomib than by either agent alone. This was associated with a marked reduction of cytoplasmic p-I κ B after FK866 and bortezomib combination treatment. Immunofluorescence staining for p-p65 further confirmed that translocation of markers of the canonical NF- κ B pathway from the cytoplasm compartment to nucleus is

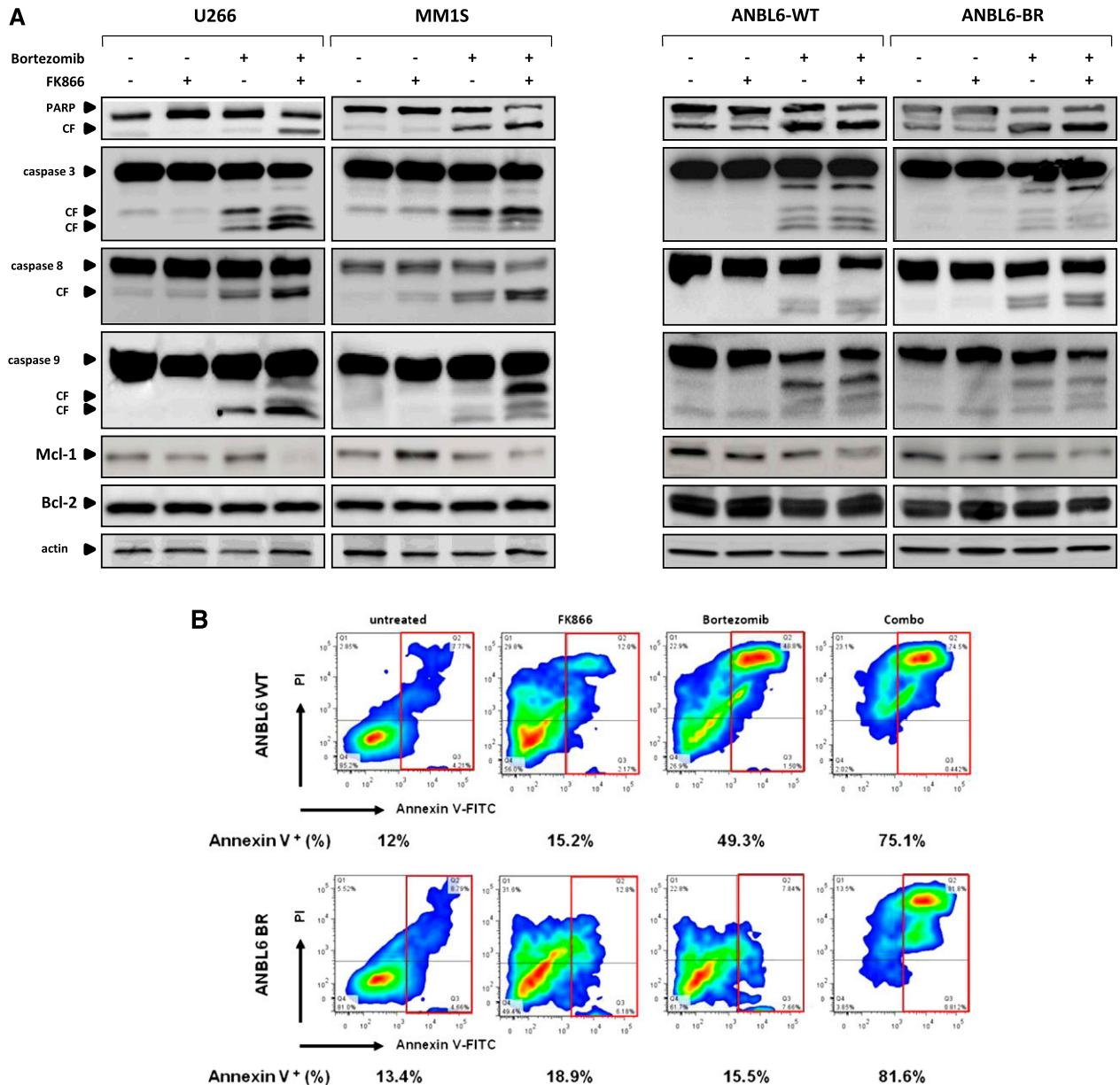


Figure 3. Mechanisms mediating the anti-MM activity of FK866 plus bortezomib. (A) MM-1S, U266, ANBL6/WT, and ANBL6/BR cells were pretreated with or without low-dose FK866 (3 nM) for 24 hours, and then bortezomib (2 nM) was added for an additional 24 hours. Cells were then harvested, and whole-cell lysates were subjected to immunoblot analysis using anti-PARP, anti-caspase 3, anti-caspase 8, anti-caspase 9, anti-Mcl-1, anti bcl-2, or anti-actin antibodies. (B) Bortezomib-sensitive (ANBL6/WT) and bortezomib-resistant (ANBL6/BR) cells were treated with FK866 (3 nM), bortezomib (2 nM), or combined therapy for 72 hours, followed by Annexin V/PI staining and flow cytometry analysis. CF, cleaved fragment; FL, full length.

completely abrogated by the drug combination in comparison with single-agent treatment (Figure 6F).

Collectively, our data therefore suggest that addition of FK866 to bortezomib in MM cells suppresses proteasome activities, thereby inhibiting degradation of misfolded/oligomerized toxic proteins, blocking NF- κ B pathway activation, and triggering MM cell death.

FK866 plus bortezomib triggers synergistic inhibition of human MM cell growth in vivo

Having shown that low doses of FK866 enhance the anti-MM effect of bortezomib in vitro, we next evaluated this synergism in vivo using the human plasmacytoma MM1S xenograft mouse model. In our previous study, we showed that high doses of FK866 alone are

effective in a MM xenograft model.⁷ To assess for synergistic cytotoxicity in vivo, we used low doses of either bortezomib (0.5 mg/kg biweekly) or FK866 (30 mg/kg daily for 4 days a week administered intraperitoneally). As seen in Figure 7A, low doses of either agent had minimal effect on tumor growth, which increased as in control mice. Importantly, when bortezomib was combined with FK866, there was a significant reduction in tumor growth in relation to untreated mice noted as early as week 1 and confirmed at the end of therapy ($P = .0045$ and $P < .001$, respectively). Furthermore, combined treatment was well tolerated, with the single daily FK866 administration better tolerated than the previous described twice-a-day schedule^{7,8}; no significant weight loss or neurological changes (data not shown) were observed. The median overall survival of FK866-treated and low-dose bortezomib-treated

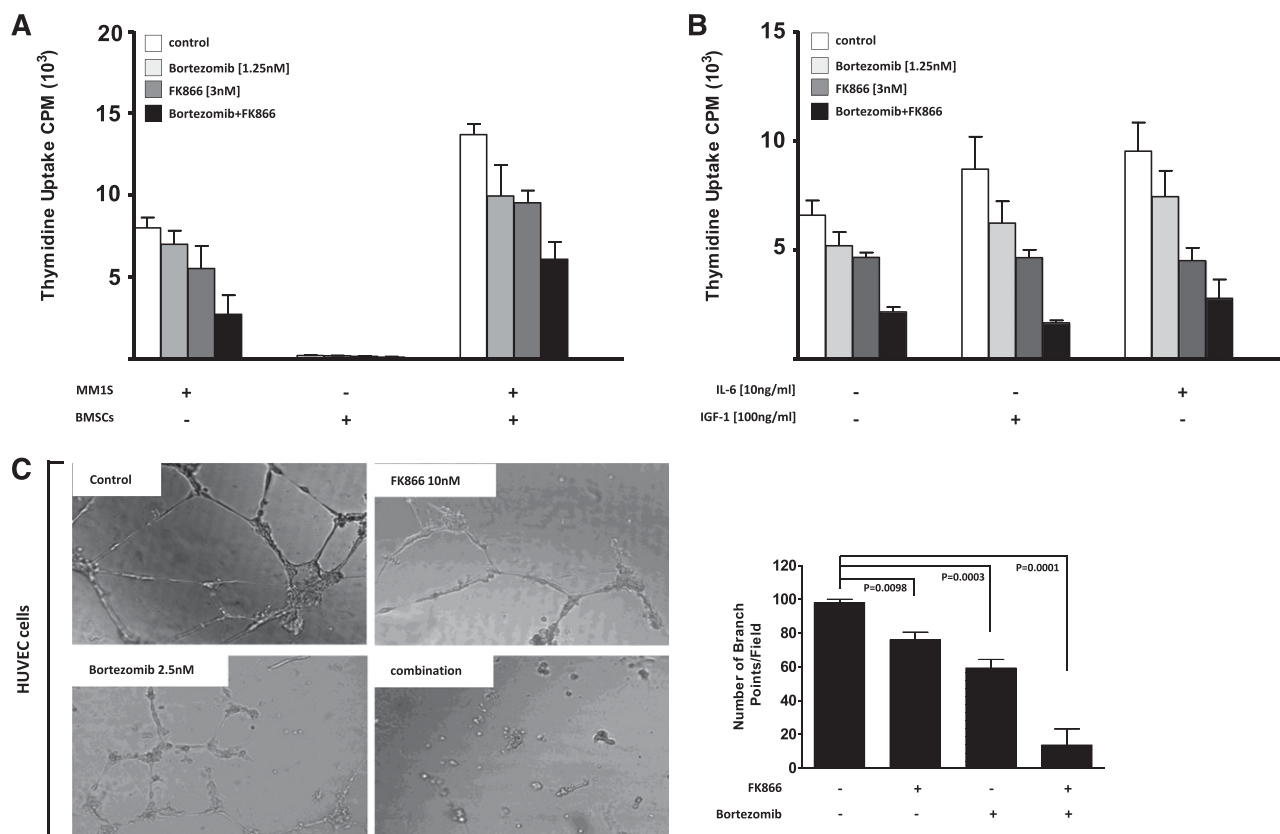


Figure 4. Combined low doses of FK866 and bortezomib overcome the survival advantage conferred by the BM microenvironment and inhibit in vitro capillary-like tube formation. (A) MM1S cells were cultured for 72 hours in BMSC-coated or -uncoated wells with control media, FK866, bortezomib, or FK866 plus bortezomib. Cell proliferation was assessed by [³H]thymidine incorporation assay. Data are mean \pm SD of triplicate samples. Error bars represent SD. (B) MM1S cells were treated with FK866, bortezomib, or their combination in the presence or absence of rhIL-6 (10 ng/mL) or rhIGF-1 (100 ng/mL) for 72 hours; DNA synthesis was then determined by [³H]thymidine uptake. The results are mean \pm SD of triplicate samples. (C) HUVEC were treated with FK866 (10 nM), bortezomib (2.5 nM), or their combination for 8 hours and then assessed for in vitro angiogenesis using Matrigel capillary-like tube structure formation assay. Endothelial cell tube formation was analyzed by microscopy (magnification: $\times 40$ /DIC NA 0.75). Image is representative of 3 experiments with similar results (left). Bar graph represents quantification of tube formation in left panel in response to indicated stimuli: branch points in several random views/well were counted, values were averaged, and statistical significance of differences was measured using the Student *t* test (right). Error bars represent SD. CPM, [³H]thymidine incorporation.

mice was significantly longer than for vehicle-treated mice (37 vs 20 days; $P = .007$) or for mice treated with either drug alone (28 days for bortezomib and 22 days for FK866) (Figure 7B). Together, these findings suggest that combining FK866 with bortezomib markedly reduces tumor growth and is well tolerated in vivo.

We also examined the effect of this combination in vivo by caspase 3 staining of human MM xenografts harvested from treated mice. We observed that combination therapy, but not treatment with either agent alone, dramatically increased the number of cleaved caspase-3 positive MM cells (Figure 7C). A significant decrease in proliferation marker Ki67 was also noted in tumor sections from combination-treated-mice in relation to mice receiving treatment with either drug alone or vehicle.

Because our in vitro data indicated antiangiogenic activity of FK866 plus bortezomib, we next evaluated paraffin-embedded sections of harvested xenografted tumors by immunohistochemistry for CD31, a marker of angiogenesis. As is shown in Figure 7C, in vivo treatment with FK866 plus bortezomib triggered a marked decrease of CD31-positive cells in comparison with single-agent or vehicle treatment, confirming in vivo antiangiogenic activity of the combination.

Finally, consistent with in vitro results, a significant reduction of Mcl-1 protein level was observed in tumor harvested from combination-treated mice in comparison with mice treated with either drug alone or vehicle (Figure 7D).

Together, these results demonstrate potent in vivo anti-MM activity of FK866 combined with bortezomib at doses that are well

tolerated, providing the framework for clinical evaluation of this combination in the treatment of MM.

Discussion

Currently available anti-MM therapies have remarkably improved patient outcome, but resistance to therapy develops even to novel therapies, and 5-year survival remains at 40%.³⁷⁻³⁹ Therefore, there is an urgent need to define the biologic mechanism of drug resistance, both to enhance use of existing treatments and to facilitate the design of novel single-agent and combination therapies. We have recently demonstrated that Namp1, a key enzyme involved in NAD⁺ metabolism, is essential for maintenance of MM cell viability.^{6,7} Importantly, selective Namp1 inhibition by FK866 induced autophagic MM cell death both in vitro and in vivo. Similar antitumor activity of this drug has been reported in a broad range of malignancies,^{26,40-43} followed by several phase 1/2 clinical trials (www.clinicaltrials.gov). Furthermore, Namp1 is associated with drug resistance in cancer cell lines and human tumor tissues,⁴⁴ suggesting that inhibition of Namp1 may restore sensitivity and overcome drug resistance.

In the current study, we first observed higher Namp1 mRNA level in gene expression profiling (GEP) of bortezomib-resistant patients, which is associated with poor survival. This observation led us to examine the role of Namp1 in bortezomib resistance. Importantly, we showed that the combination of FK866 and

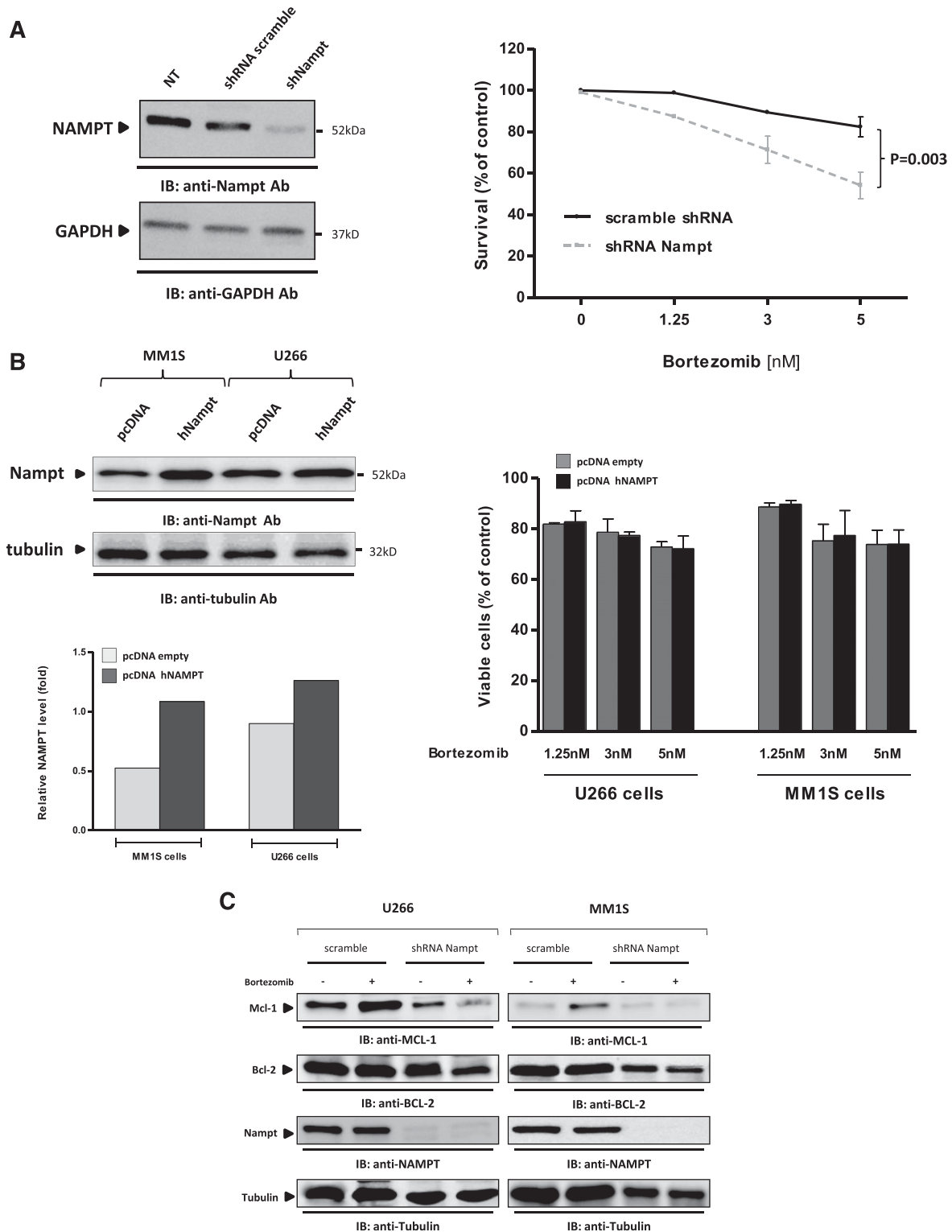


Figure 5. Role of Nampt in modulating response to bortezomib. (A) MM1S cells were infected with either lentiviral construct expressing control scrambled or shRNA targeting Nampt. Total protein extracts were then subjected to immunoblot analysis with anti-Nampt or anti-GAPDH antibodies (left). The effect of Nampt knockdown on bortezomib response was assessed by measuring viability of infected cells (with shRNA scramble or targeting Nampt) after bortezomib treatment (1.25–5 nM) by using PI staining followed by FACS analysis (right). (B) Representative immunoblot images showing Nampt overexpressed in MM1S and U266 cells. Antitubulin monoclonal antibody served as loading control (top). Relative expression of Nampt protein was calculated by taking the ratio of the densitometry signal for Nampt to tubulin in each sample using Image J software (bottom). Cells overexpressing Nampt were subjected to bortezomib treatment of 24 h, and then viability was measured by MTT analysis (right). (C) U266 and MM1S cells were infected with a specific lentiviral shNampt or scramble control and then treated with 2 nM bortezomib for 24 hours. Thereafter, cells were used for cell lysates preparation, and Nampt, Mcl-1, bcl-2, and tubulin were detected by immunoblotting.

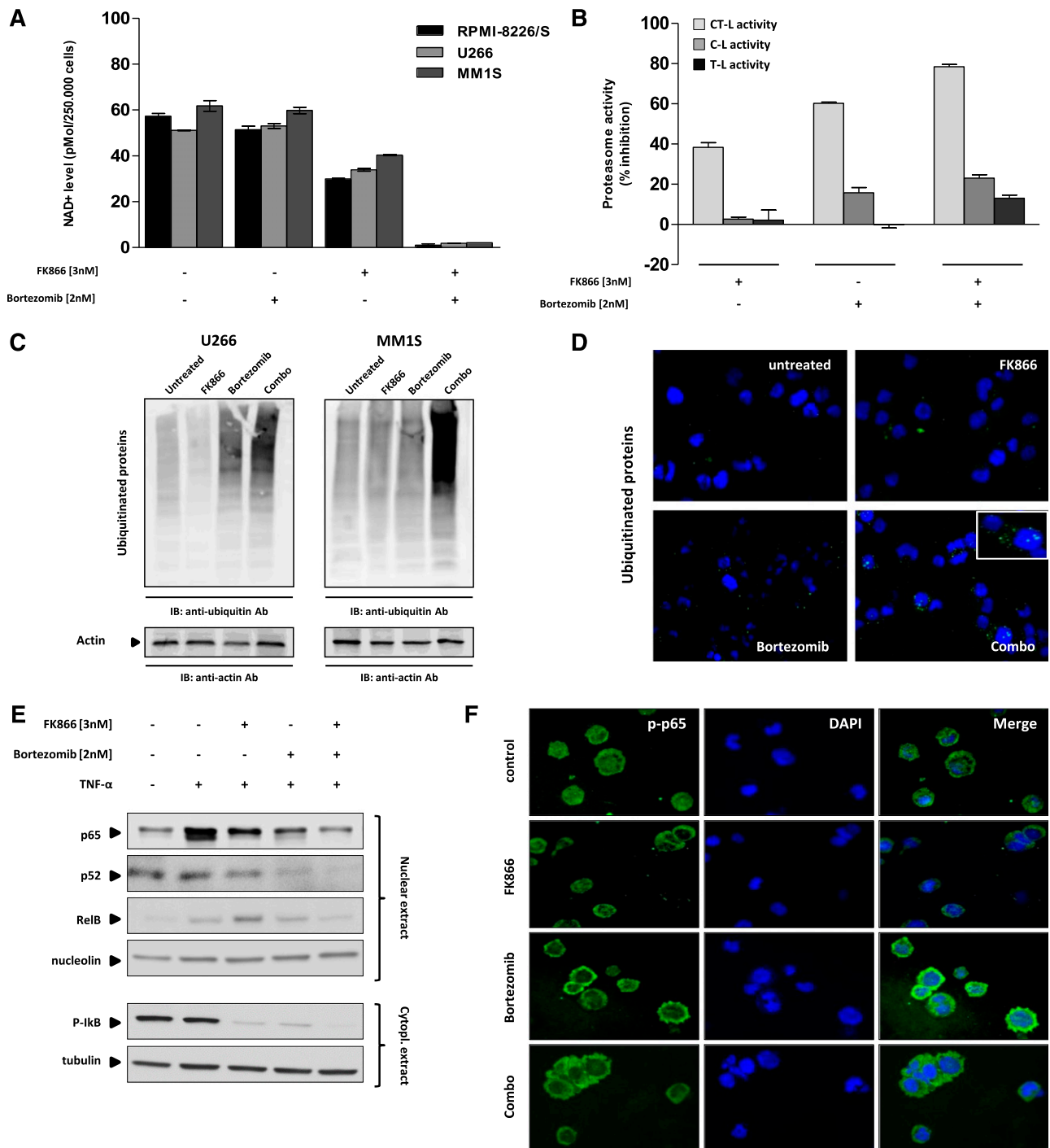


Figure 6. Combination treatment inhibits UPS and NF-κB pathway in MM cells. (A) MM cell lines were treated with FK866 (3 nM), bortezomib (2 nM), or combined therapy for 3 hours. Cells were then harvested, and intracellular NAD⁺ level was measured using an enzyme cyclic assay and normalized to total cell number. Data are mean ± SD of 2 independent experiments. (B) MM1S cells were treated with FK866 (3 nM) for 48 hours, and bortezomib (2 nM) was added for the last 6 hours. Cell extracts were then analyzed for 20S proteasome activities (CT-L, C-L, and T-L). Results are percentage inhibition of proteasome activities in drug in comparison with vehicle control-treated cells. Data are representative of 3 independent experiments. (C) MM1S and U266 cells were treated with FK866 (3 nM), bortezomib (2 nM), or combined therapy for 24 hours. Whole-cell lysates were then immunoblotted using antiubiquitin and antiactin Abs. Blots shown are representative of 3 independent experiments. (D) MM1S cells were treated with FK866 (3 nM), bortezomib (2 nM), or their combination for 24 hours. Cells were then fixed and stained with 4',6-diamidino-2-phenylindole (blue) and antiubiquitin Ab. (E) MM1S cells were cultured with FK866 (3 nM), bortezomib (2 nM), or their combination for 6 hours, with TNF-α (10 ng/mL) added for the last 20 minutes. Cytoplasmic and nuclear extracts were subjected to western blotting using specific antibody for analysis of NF-κB canonical (anti-p-NF-κBp65 and -p-IκB) and noncanonical (-NF-κBp52, -RelB) activity. (F) MM1S cells were cultured with FK866 (3 nM), bortezomib (2 nM), or the combination for 6 hours, with TNF-α (10 ng/mL) added for the last 20 minutes. Immunocytochemical analysis was performed using anti-pospho-NF-κBp65 antibody. DAPI (4',6-diamidino-2-phenylindole) was used to stain nuclei.

bortezomib, at concentrations of either agent alone that are inactive, triggered marked cytotoxicity against a panel of MM cell lines. This cytotoxicity triggered by combined treatment was noted in MM cell

lines sensitive and resistant to conventional and novel therapies, including Dex-sensitive MM1S, Dex-resistant MM1R, and bortezomib-resistant ANBL6-BR cells. This combination, but

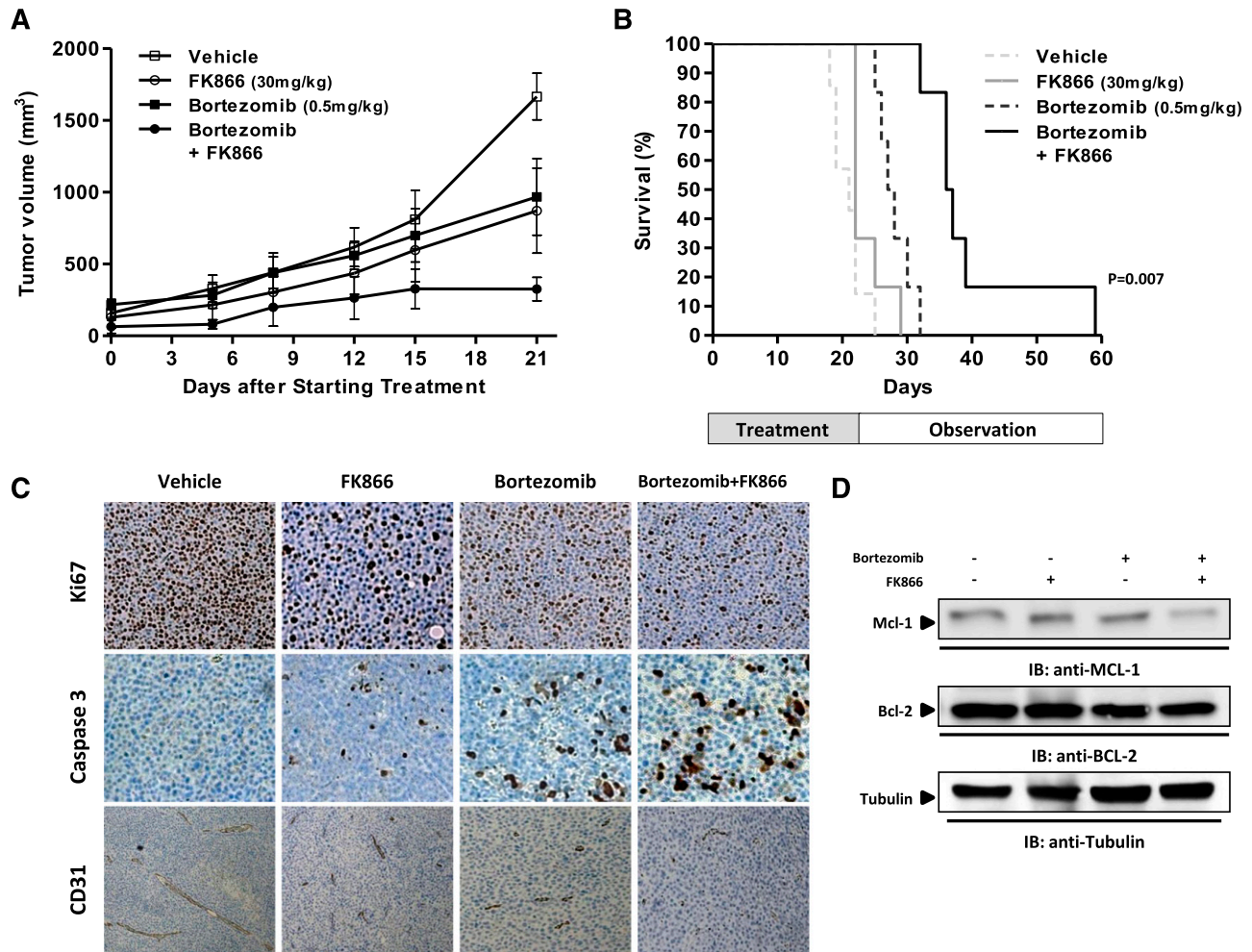


Figure 7. FK866 plus bortezomib trigger synergistic inhibition of human MM cell growth in vivo. (A) Average and SD of tumor volume (mm³) from groups of mice (n = 7 per group) versus time (days) when tumor was measured. MM1S cells (5 × 10⁶ in 100 μL of serum-free RPMI-1640 medium) were implanted in the flank of CB17 SCID mice. After tumor detection, mice were randomized to intraperitoneal treatment with vehicle, FK866, bortezomib, or their combination at the indicated doses over 3 weeks. A significant decrease in tumor growth was noted in combination-treated mice versus vehicle-treated mice (P = .0045 after the first week and P < .001 at the end of treatment). Data are mean tumor volume ± SD. Error bars represent mean ± SD. (B) Kaplan–Meier survival plot showing survival for mice treated with vehicle, FK866, bortezomib, or their combination at the indicated concentrations. FK866 plus bortezomib-treated mice show significantly increased survival (P = .007) in comparison with vehicle-treated mice. The mean overall survival was 20 days in the vehicle-treated cohort versus 37 days in the combination-treated cohort. (C) Micrographs show tumors sectioned on day 30 (endpoint) from vehicle-, FK866- (30 mg/kg), bortezomib- (0.5 mg/kg), or combination-treated mice immunostained for Ki-67, caspase 3, or CD31 expression. Photographs are representative of 2 mice receiving each treatment. (D) Cell lysates were prepared from tumor tissues harvested from treated and untreated mice and then analyzed by western blot analysis for Mcl-1 and Bcl-2 protein level.

not low doses of FK866 or bortezomib alone, also overcomes the MM-cell growth advantage conferred by cytokines and BM microenvironment in vitro. Finally, we observed similar responses in bortezomib-resistant patient MM cells, as well as in a human MM xenograft model. The marked antitumor activity of this combination, coupled with the lack of its effect on PBMCs, suggests a favorable therapeutic index.

Mechanistic studies showed that the anti-MM activity of this combination is due to caspase activation and Mcl-1 downregulation, which result in apoptotic cell death, distinct from the autophagic cell death previously observed with single-agent FK866 treatment.^{7,8,45} The lack of autophagy triggered by combined therapy suggests that lower doses of drugs used here are unable to activate or sustain autophagy but can activate apoptotic signaling.

It has been demonstrated that mechanisms of resistance to bortezomib may be multifactorial, including mutations in or overexpression of proteasome subunits, as well as upregulation of antiapoptotic proteins such as Bcl-2 or Mcl-1.^{46,47} Here we postulated that downregulation of Mcl-1 and Bcl-2 observed in parental MM

cells, as well as in their bortezomib-resistant counterparts after combination treatment, contributes to synergistic interactions between FK866 and bortezomib. Indeed, Nampt depletion by RNAi was associated with downregulation of Mcl-1 induction by bortezomib and significantly increased bortezomib-induced apoptosis. These data identify Nampt as an important mechanism mediating upregulation of Mcl-1 by proteasome inhibition.

We also showed that FK866 plus bortezomib-induced MM cell apoptosis is associated with a significant deregulation of UPS and NF-κB pathways, which play crucial roles in the pathogenesis of MM. Combined therapy triggers intracellular NAD⁺ depletion with subsequent ATP shortage, thereby inhibiting ATP-dependent 20S proteasomal activities. Importantly, our mechanistic studies indicate that addition of FK866 to bortezomib induces energy depletion with consequent inhibition of the UPS, thereby resulting in ubiquitinated protein accumulation, NF-κB inhibition, and MM cell death. The observation that Nampt plays a role in modulating sensitivity of MM cells to bortezomib was confirmed by our loss- and gain-of-function experiments, which showed a greater anti-MM

effect of bortezomib in Nampt-depleted cells than in isogenic MM cells. Finally, our in vivo MM xenograft data demonstrate that this drug combination inhibits tumor growth, with immunohistochemical analysis showing apoptosis and antiangiogenic activity, as well as prolonged host survival, further confirming the therapeutic potential of combined therapy.

Despite the great therapeutic benefit of bortezomib, development of bortezomib resistance has already stimulated research for more potent second-generation proteasome inhibitors, as well as scientifically improved combination therapies, to prevent or overcome bortezomib resistance.

In this setting, our data show that adding low doses of NAD⁺-depleting agent FK866 to bortezomib both enhances sensitivity and overcomes resistance to bortezomib. Our preclinical studies therefore provide the rationale for development of novel combination anti-MM therapy targeting NAD⁺ salvage pathway to enhance efficacy of bortezomib-based therapies in MM.

Acknowledgments

The authors thank the National Institute of Mental Health Chemical Synthesis and Drug Supply Program for generously providing FK866 for this study.

References

- Cairns RA, Harris IS, Mak TW. Regulation of cancer cell metabolism. *Nat Rev Cancer*. 2011; 11(2):85-95.
- Vander Heiden MG, Cantley LC, Thompson CB. Understanding the Warburg effect: the metabolic requirements of cell proliferation. *Science*. 2009; 324(5930):1029-1033.
- Hanahan D, Weinberg RA. Hallmarks of cancer: the next generation. *Cell*. 2011;144(5):646-674.
- Berger F, Ramírez-Hernández MH, Ziegler M. The new life of a centenarian: signalling functions of NAD(P). *Trends Biochem Sci*. 2004;29(3): 111-118.
- Houtkooper RH, Cantó C, Wanders RJ, Auwerx J. The secret life of NAD⁺: an old metabolite controlling new metabolic signaling pathways. *Endocr Rev*. 2010;31(2):194-223.
- Chiariugi A, Dölle C, Felici R, Ziegler M. The NAD metabolome—a key determinant of cancer cell biology. *Nat Rev Cancer*. 2012;12(11):741-752.
- Cea M, Cagnetta A, Fulciniti M, et al. Targeting NAD⁺ salvage pathway induces autophagy in multiple myeloma cells via mTORC1 and extracellular signal-regulated kinase (ERK1/2) inhibition. *Blood*. 2012;120(17):3519-3529.
- Cea M, Cagnetta A, Patrone F, Nencioni A, Gobbi M, Anderson KC. Intracellular NAD(+) depletion induces autophagic death in multiple myeloma cells. *Autophagy*. 2013;9(3):410-412.
- Zoppoli G, Cea M, Soncini D, et al. Potent synergistic interaction between the Nampt inhibitor APO866 and the apoptosis activator TRAIL in human leukemia cells. *Exp Hematol*. 2010;38(11):979-988.
- Pogrebniak A, Schemainda I, Azzam K, Pelka-Fleischer R, Nüssler V, Hasmann M. Chemopotentiation effects of a novel NAD biosynthesis inhibitor, FK866, in combination with antineoplastic agents. *Eur J Med Res*. 2006;11(8): 313-321.
- Yang H, Yang T, Baur JA, et al. Nutrient-sensitive mitochondrial NAD⁺ levels dictate cell survival. *Cell*. 2007;130(6):1095-1107.
- Travelli C, Drago V, Maldì E, et al. Reciprocal potentiation of the antitumor activities of FK866, an inhibitor of nicotinamide phosphoribosyltransferase, and etoposide or cisplatin in neuroblastoma cells. *J Pharmacol Exp Ther*. 2011;338(3):829-840.
- Muruganandham M, Alfieri AA, Matei C, et al. Metabolic signatures associated with a NAD synthesis inhibitor-induced tumor apoptosis identified by 1H-decoupled-31P magnetic resonance spectroscopy. *Clin Cancer Res*. 2005; 11(9):3503-3513.
- Richardson PG, Barlogie B, Berenson J, et al. A phase 2 study of bortezomib in relapsed, refractory myeloma. *N Engl J Med*. 2003;348(26): 2609-2617.
- Lonial S, Waller EK, Richardson PG, et al; SUMMIT/CREST Investigators. Risk factors and kinetics of thrombocytopenia associated with bortezomib for relapsed, refractory multiple myeloma. *Blood*. 2005;106(12):3777-3784.
- Hideshima T, Bradner JE, Wong J, Chauhan D, Richardson P, Schreiber SL, Anderson KC. Small-molecule inhibition of proteasome and aggresome function induces synergistic antitumor activity in multiple myeloma. *Proc Natl Acad Sci USA*. 2005; 102(24):8567-8572.
- Roccaro AM, Hideshima T, Raje N, et al. Bortezomib mediates antiangiogenesis in multiple myeloma via direct and indirect effects on endothelial cells. *Cancer Res*. 2006;66(1): 184-191.
- Chou TC, Talalay P. Quantitative analysis of dose-effect relationships: the combined effects of multiple drugs or enzyme inhibitors. *Adv Enzyme Regul*. 1984;22:27-55.
- Mulligan G, Mitsiades C, Bryant B, et al. Gene expression profiling and correlation with outcome in clinical trials of the proteasome inhibitor bortezomib. *Blood*. 2007;109(8):3177-3188.
- Kumatori A, Tanaka K, Inamura N, et al. Abnormally high expression of proteasomes in human leukemic cells. *Proc Natl Acad Sci USA*. 1990;87(18):7071-7075.
- Hideshima T, Richardson P, Chauhan D, et al. The proteasome inhibitor PS-341 inhibits growth, induces apoptosis, and overcomes drug resistance in human multiple myeloma cells. *Cancer Res*. 2001;61(7):3071-3076.
- Michallet AS, Mondiere P, Taillardat M, Leverrier Y, Genestier L, Defrance T. Compromising the unfolded protein response induces autophagy-mediated cell death in multiple myeloma cells. *PLoS ONE*. 2011;6(10):e25820.
- Hideshima T, Mitsiades C, Tonon G, Richardson PG, Anderson KC. Understanding multiple myeloma pathogenesis in the bone marrow to identify new therapeutic targets. *Nat Rev Cancer*. 2007;7(8):585-598.
- Podar K, Tai YT, Davies FE, et al. Vascular endothelial growth factor triggers signaling cascades mediating multiple myeloma cell growth and migration. *Blood*. 2001;98(2):428-435.
- Bataille R, Chappard D, Marcelli C, et al. Recruitment of new osteoblasts and osteoclasts is the earliest critical event in the pathogenesis of human multiple myeloma. *J Clin Invest*. 1991; 88(1):62-66.
- Hasmann M, Schemainda I. FK866, a highly specific noncompetitive inhibitor of nicotinamide phosphoribosyltransferase, represents a novel mechanism for induction of tumor cell apoptosis. *Cancer Res*. 2003;63(21):7436-7442.
- Bruzzzone S, Fruscione F, Morando S, et al. Catastrophic NAD⁺ depletion in activated T lymphocytes through Nampt inhibition reduces demyelination and disability in EAE. *PLoS ONE*. 2009;4(11):e7897.
- Arendt CS, Hochstrasser M. Identification of the yeast 20S proteasome catalytic centers and subunit interactions required for active-site formation. *Proc Natl Acad Sci USA*. 1997;94(14): 7156-7161.
- Heinemeyer W, Fischer M, Krimmer T, Stachon U, Wolf DH. The active sites of the eukaryotic 20S proteasome and their involvement in subunit precursor processing. *J Biol Chem*. 1997;272(40): 25200-25209.

Authorship

Contribution: A.C. and M.C. designed and performed research, analyzed data, and wrote the paper; T.C. performed animal work; C.A., Y.-T.T., T.H., D.C., and M.F. provided reagents, analytic tools, and input to studies; M.G., F.P., A.N., P. R., and N.M. provided MM patient samples and critically evaluated the manuscript; and K.C.A. critically evaluated and edited the manuscript.

Conflict-of-interest disclosure: The authors declare no competing financial interests.

Correspondence: Michele Cea, Department of Medical Oncology, Dana-Farber Cancer Institute, M551, 450 Brookline Ave, Boston, MA 02115; e-mail: michele_cea@dfci.harvard.edu; or Kenneth C. Anderson, Department of Medical Oncology, Dana-Farber Cancer Institute, M557, 450 Brookline Ave, Boston, MA 02115; e-mail: kenneth_anderson@dfci.harvard.edu.

30. Chauhan D, Catley L, Li G, et al. A novel orally active proteasome inhibitor induces apoptosis in multiple myeloma cells with mechanisms distinct from Bortezomib. *Cancer Cell*. 2005;8(5):407-419.
31. Lightcap ES, McCormack TA, Pien CS, Chau V, Adams J, Elliott PJ. Proteasome inhibition measurements: clinical application. *Clin Chem*. 2000;46(5):673-683.
32. Cao B, Mao X. The ubiquitin-proteasomal system is critical for multiple myeloma: implications in drug discovery. *Am J Blood Res*. 2011;1(1):46-56.
33. Chauhan D, Uchiyama H, Akbarali Y, et al. Multiple myeloma cell adhesion-induced interleukin-6 expression in bone marrow stromal cells involves activation of NF-kappa B. *Blood*. 1996;87(3):1104-1112.
34. Feinman R, Koury J, Thames M, Barlogie B, Epstein J, Siegel DS. Role of NF-kappaB in the rescue of multiple myeloma cells from glucocorticoid-induced apoptosis by bcl-2. *Blood*. 1999;93(9):3044-3052.
35. Markovina S, Callander NS, O'Connor SL, et al. Bortezomib-resistant nuclear factor-kappaB activity in multiple myeloma cells. *Mol Cancer Res*. 2008;6(8):1356-1364.
36. Watson M, Roulston A, Bélec L, et al. The small molecule GMX1778 is a potent inhibitor of NAD+ biosynthesis: strategy for enhanced therapy in nicotinic acid phosphoribosyltransferase 1-deficient tumors. *Mol Cell Biol*. 2009;29(21):5872-5888.
37. Kumar SK, Rajkumar SV, Dispenzieri A, et al. Improved survival in multiple myeloma and the impact of novel therapies. *Blood*. 2008;111(5):2516-2520.
38. Raab MS, Podar K, Breitkreutz I, Richardson PG, Anderson KC. Multiple myeloma. *Lancet*. 2009;374(9686):324-339.
39. Venner CP, Connors JM, Sutherland HJ, et al. Novel agents improve survival of transplant patients with multiple myeloma including those with high-risk disease defined by early relapse (<12 months). *Leuk Lymphoma*. 2011;52(1):34-41.
40. Nahimana A, Attinger A, Aubry D, et al. The NAD biosynthesis inhibitor APO866 has potent antitumor activity against hematologic malignancies. *Blood*. 2009;113(14):3276-3286.
41. Holen K, Saltz LB, Hollywood E, Burk K, Hanauske AR. The pharmacokinetics, toxicities, and biologic effects of FK866, a nicotinamide adenine dinucleotide biosynthesis inhibitor. *Invest New Drugs*. 2008;26(1):45-51.
42. Billington RA, Genazzani AA, Travelli C, Condorelli F. NAD depletion by FK866 induces autophagy. *Autophagy*. 2008;4(3):385-387.
43. Cea M, Zoppoli G, Bruzzone S, et al. APO866 activity in hematologic malignancies: a preclinical in vitro study. *Blood*. 2009;113(23):6035-6037.
44. Figueira MA, Carraro DM, Brentani H, et al. Gene expression profile associated with response to doxorubicin-based therapy in breast cancer. *Clin Cancer Res*. 2005;11(20):7434-7443.
45. David E, Kaufman JL, Flowers CR, et al. Tipifarnib sensitizes cells to proteasome inhibition by blocking degradation of bortezomib-induced aggregates. *Blood*. 2010;116(24):5285-5288.
46. Mujtaba T, Dou QP. Advances in the understanding of mechanisms and therapeutic use of bortezomib. *Discov Med*. 2011;12(67):471-480.
47. Walsby EJ, Pratt G, Hewamana S, et al. The NF-kappaB inhibitor LC-1 has single agent activity in multiple myeloma cells and synergizes with bortezomib. *Mol Cancer Ther*. 2010;9(6):1574-1582.